Description of TEAM Workshop Problem 33.a: Experimental Validation of Magnetic Local Force Formulations.

Olivier Barré, Pascal Brochet, *Member, IEEE*, Michel Hecquet.

***Abstract*— This paper describes an experiment whose goal is to underline the accuracy of methods that are able to induce local force formulations associated to a magnetic field. First of all, a magnetic structure with a large air gap is used to generate a magnetic field. A specimen with low relative permeability is placed in this air-gap and its deformation is observed. The geometry of all parts is well described; physical properties of all materials are given. These data allow anyone to model this test bench, predict its behaviour with simulations and compare calculated results to experiments.**

***Index Terms*—Electromagnetic forces, Electromagnetic fields, Experimental validation and energy methods.**

I. Introduction

When the calculation of local forces induced by magnetic field is required, different formulations can be used [1] [3] [4] [5] [10] [11]. Choosing the proper formulation is not easy [2] [8]. First of all, global measurement will not provide adequate results to validate a local formulation. Different force distributions can provide the same total force. Hence, it is necessary to find a new method to test local formulations. The deformation of a body under external stress is totally linked to this stress distribution [6] [7]. But the difficulty is the need of a material that is able to provide visible deformation under low strengths [9] [12].

II. Test bench overview.

When a magnetic body is submitted to an external magnetic field, magnetic forces act on its boundary. Such a stress distribution induces mechanical deformations. The basic idea is to provide visible deformation on a specimen with well-chosen physical properties (Fig. 1). In this experiment, a deformation occurs because the specimen is placed in a non symmetric position in the air gap.

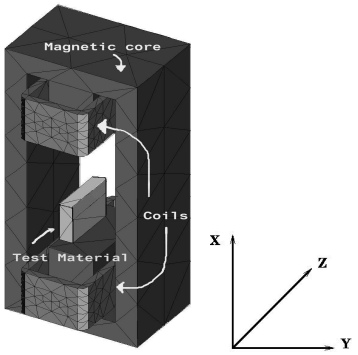

Fig. 1. A magnetic core associated with coils imposes a magnetic field distribution that is approximately constant along the Z-direction. A test material is set in the air gap.

III. Magnetic Field Generation.

Generating a magnetic field is easy, but to calculate the field distribution is not always easy. Electric current in coils is used as magnetic source. The coil is designed for up to 250 copper wires loops. Its geometry is given in the Fig.2.

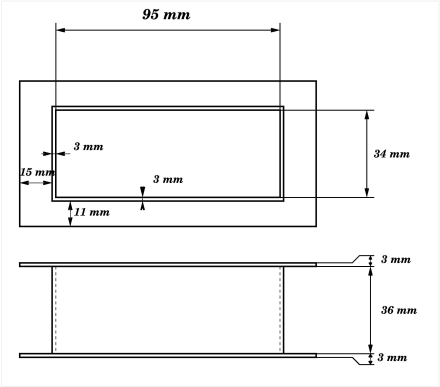

Fig. 2. Coil holder geometry.

Copper wires turns are placed in the holder as shown in the Fig. 3. It is not necessary to entirely fill this holder. Each of the two coils only contains 150 copper turns; it can be modelled as a single coil whose geometry is presented in Fig 4.

O. Barré. is with the Laboratoire D'Electrotechnique et d'Electronique de Puissance of Ecole Centrale de Lille, Cité Scientifique, BP-48, 59651 Villeneuve d'Ascq Cedex, France (Phone : 33-03-20335385 ; Fax : 33-03-20335454 ; e-mail: olivier.barre@ec-lille.fr).

P. Brochet. is with the Laboratoire D'Electrotechnique et d'Electronique de Puissance of Ecole Centrale de Lille, Cité Scientifique, BP-48, 59651 Villeneuve d'Ascq Cedex, France (e-mail: pascal.brochet@ec-lille.fr).

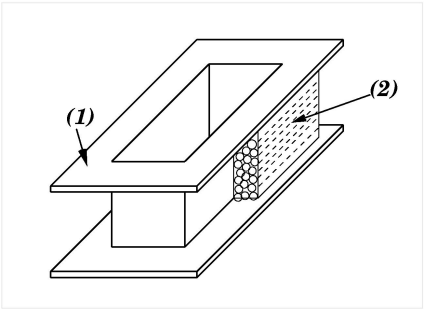

Fig. 3. Copper wires (2) are rolled around the holder (1).

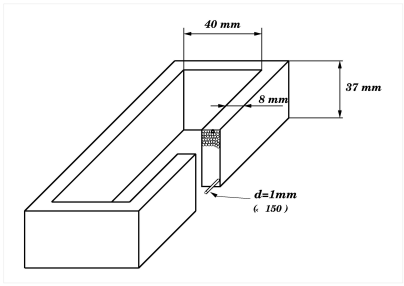

Fig. 4. Coil geometry.

A magnetic core is built from parts of a transformer. Even if using such parts does not allow a high freedom about the final geometry of the core, this one is well known. Two different parts are used and their geometries are given in the Figs. 5 and 6.

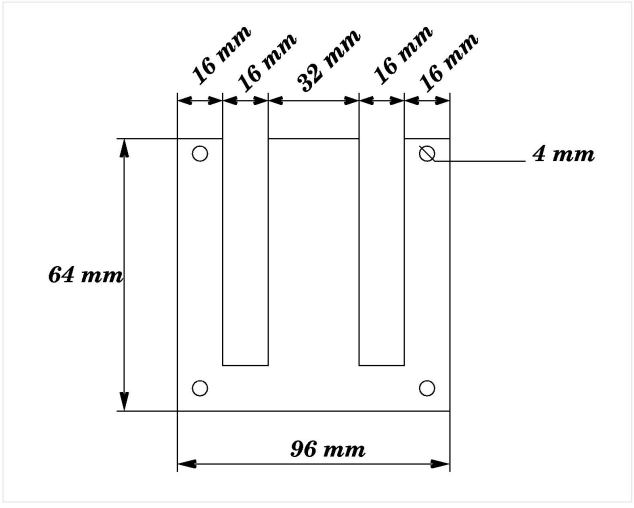

Fig. 5. Part (A)

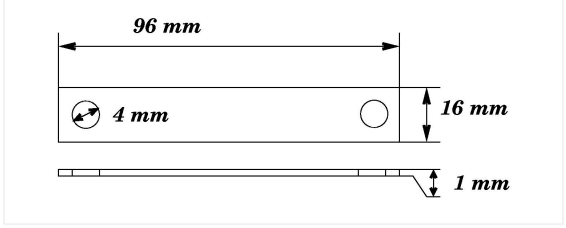

Fig. 6. Part (B)

Those parts are assembled to build the magnetic core shown in the Fig. 7. The screws and the bolts used for the assembly are of iron and the magnetic core can be modelled without being broken up into subsets. The relative permeability of all the component is assumed to be high (greater than 1000).

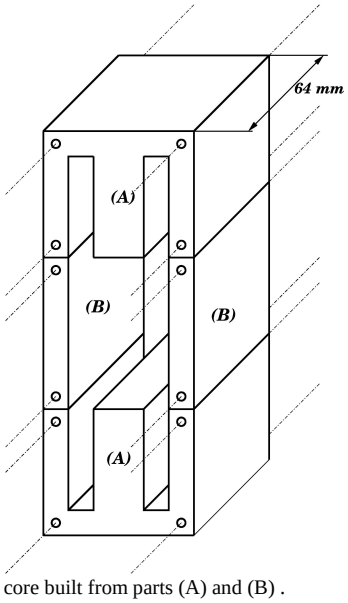

Fig. 7. Magnetic core built from parts (A) and (B) .

IV. Specimen.

A test material with low relative permeability is used for this experiment. Many magnetic local force formulations are available and when they are applied to such material, they provide results very different from each other. Moreover, while the geometry contains singular points, it is necessary to undervalue the local force effect in any area where the field distribution is not reliable. Therefore, the specimen is tall and a relative permeability under 5 is preferred. The geometry of this specimen is given in Fig. 8.

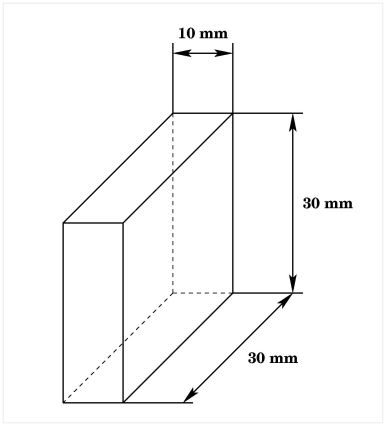

Fig. 8. Specimen geometry in magnetic experiment.

V. PHYSICAL PROPERTIES OF TEST MATERIAL.

V.a) Mechanical properties.

A compression test is used to measure the Young modulus for this material (Fig. 9). Water is its most important component; its volume is kept constant during any deformation. Hence, the Poisson coefficient can be set to 0.5. Experimental data of Fig. 10 indicate, with good accuracy, that the Young modulus is 11 000 N/m².

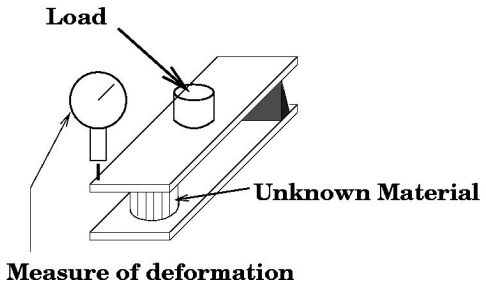

Fig. 9. Test bench associated to the Young modulus measurement.

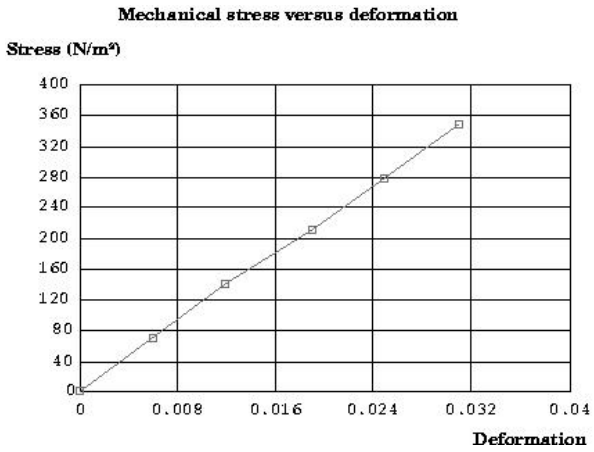

Fig. 10. Experimental results providing an evaluation of the Young modulus.

V.b) Magnetic properties.

Comparison between air and the test material is done using a ferromagnetic core with two coils. A third coil is used to give information about the magnetic flux in the core when a 0.5 A alternative current is set (Fig. 11).

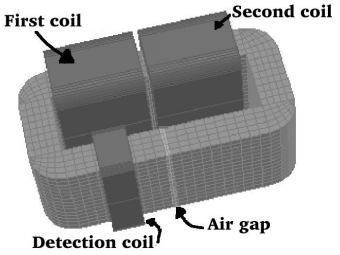

Fig. 11. Experimental test bench used to measure relative permeability.

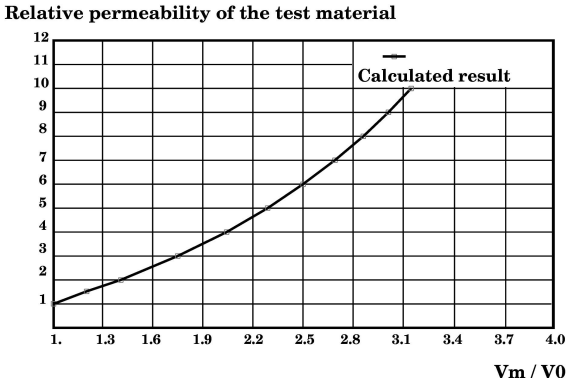

Fig. 12. Calibration curve providing relative permeability of the test material using Vm/V0.

A magnetostatic 3D model of this device is used to provide a calibration curve taking flux leakage into account. Applying an alternative current at very low frequencies (50 Hz), two measurements are done: First, the voltage delivered by the detection coil without test material in the air-gap, denoted by V0, and second, the voltage delivered when the air gap is filled with test material, denoted by Vm. With Vm/V0, Fig. 12 gives the relative permeability. For the experiment, V0=1.05 V and Vm=1.63 V, hence the test material relative permeability is: μ_r=2.5 . In summary, the material properties are given below:

E=11000N/m^2	Young modulus	(+/-10%)
ν=0.5	Poisson coefficient	
μ_r=2.5	Relative permeability	(+/-3%)

VI. EXPERIMENTAL RESULTS.

A camera with macro-photography lens is used to measure the deformation of the specimen under magnetic forces. A direct current is set in the coils and two photographs are taken as explained in Fig. 13. First, without any power supply, and second, when the coils are supplied. A comparison gives the deformation of the specimen.

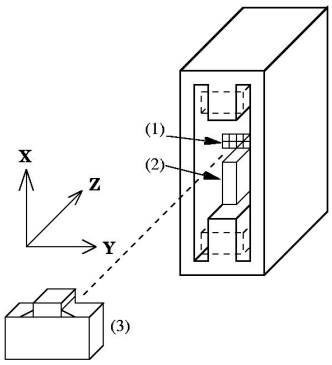

Fig. 13. Under magnetic forces, a deformation of the specimen (2) is observed. With a fixed gauge (1) and photographs (3) it is possible to measure the displacement of the top of the specimen. The gauge is graduated with 1 mm square.

0.5, 1.0, 1.5 A direct currents in coils.

Fig. 14. 0.5 A direct current is set in the coil and a displacement of 0.3 mm is measured as gauge is graduated with 1 mm square.

Fig. 15. 1.0 A direct current is set in the coil and a displacement of 0.8 mm is measured as gauge is graduated with 1 mm square..

Fig. 16. 1.5 A direct current is set in the coil and a displacement of 1.7 mm is measured as gauge is graduated with 1 mm square..

Looking at Figs. 14, 15 and 16, straightforward deformations appear. The displacement observed in the first experiment (Fig. 14) is very low and it cannot be considered accurate enough. Notice that photographs are enlarged to be exploited and we can consider a measurement error of 0.1 mm.

VII. NUMERICAL RESULTS.

The local forces density (1) provided by the energy method is used to calculate the deformation under the experimental conditions. Simulations are used to calculate the magnetic field distribution in the air-gap (with the specimen inside). The OPERA 2D/3D, a FE package, provides the results. This distribution is used to calculate the magnetic stress on the specimen. Finally, this strains distribution is used to calculate the deformation of the body (Fig. 17).

$$\vec{F}_n = \left[\frac{1}{2} \frac{1}{\mu_0} \left(1 - \frac{1}{\mu_r} \right) B_n^2 + \frac{1}{2} \mu_0 (1 - \mu_r) H_t^2 \right] \vec{n} \qquad (1)$$

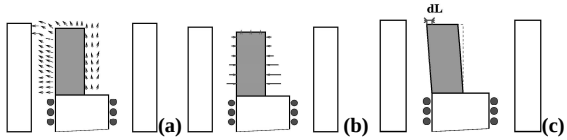

Fig. 17. (a) Field distribution, (b) example of magnetic force distribution and (c) body deformation.

With the simulation of the whole process, the predicted deformation associated to each value of direct current in the coil can be obtained (Figs. 18, 19 and 20).

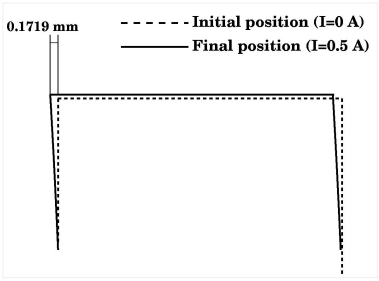

Fig. 18. 0.5 A direct current is set in the coil and a displacement of 0.1719 mm is predicted.

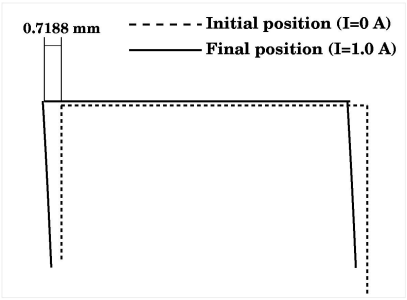

Fig. 19. 1.0 A direct current is set in the coil and a displacement of 0.7188 mm is predicted.

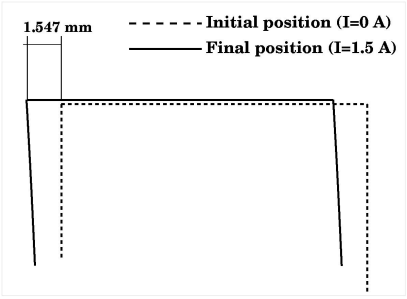

Fig. 20. 1.5 A direct current is set in the coil and a displacement of 1.547 mm is predicted.

VIII. Magnetic flux measurements.

Magnetic flux density is measured in the air-gap and those values are compared to values predicted by the 2D simulation (I=1.5 A). These values are given at the end of the study because they can only be used as information. Fig. 21 is the reference to the measurement and Fig. 22 is the result of the comparison. The position of the probe is measured manually and the accuracy is about +/- 1 mm. This means that if the measured position of the probe is x1 mm and y1 mm, the measured flux density must be compared not only to the flux density calculated at x1 and y1 but also to the flux density calculated at x1-1mm, y1-1mm, x1+1mm, y1+1mm... Hence, it appears that the measured values are values that are in agreement with the computed values if the accuracy of the position of the probe is take into account.

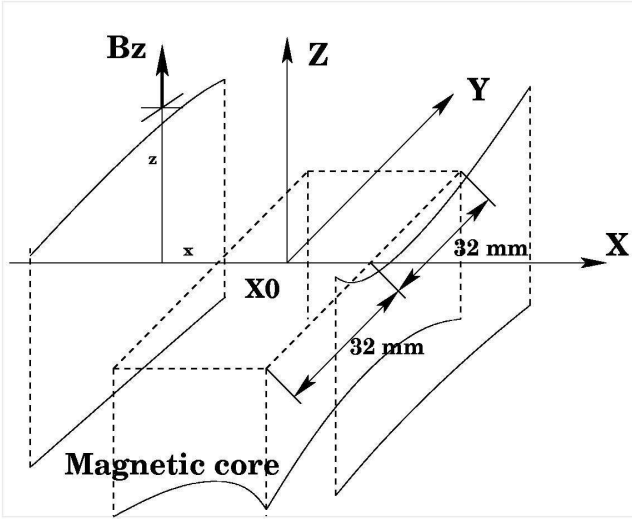

Fig. 21. Reference coordinate system about measurement of Bz intensity at several point referenced with their position in this referential.

x (m)	z (m)	Bz (mT) (calculated value)	BZ (mT) (mesured value)	(relative error)
−0.025	0.013	3.76	3.67	2%
−0.009	0.013	7.54	6.87	8%
−0.025	0.023	2.11	2.21	5%
−0.009	0.023	4.83	4.31	10%
−0.0025	0.038	1.39	1.34	4%
−0.009	0.038	2.92	2.72	7%
(1)	(2)	(3)	(4)	(5)

Fig. 22. Comparison between measurements and results of a 2D simulation. (1) and (2) are the probe coordinates. (3) and (4) are the magnetic flux density. (5) is the relative error in percent between these values. This error disappears if the accuracy of the position of the probe is taken into account.

IX. Conclusion.

In conclusion, the accuracy of different local force formulations can be tested with this bench. The precision of the relative permeability is about 3% and the accuracy of the Young modulus is about 10 %. The deformations, due to the stress distribution predicted by the energy method, are given as an example. It is shown that the energy principle is accurate and takes well into account the behaviour of materials under external magnetic field.

References

[1] T. Kabashima, A. Kawahara, T. Goto, “Force calculation using magnetizing currents“, IEEE Transaction on magnetics, Vol 24, N°1, Januray 1988, pp 451-454

[2] W. Muller, “Comparison of different methods of force calculation”, IEEE Transaction on magnetics, Vol 26, N°2, March 1990, pp 1058-1061.

[3] Z. Ren, B. Ionescu, M. Besbes and A. Razek, “Calculation of mechanical deformation of magnetic materials in electromagnetic devices”, IEEE Transaction on magnetics, Vol. 31. N°3 May 1995., pp 1873-1876.

[4] J.D. Jacobson, S.H. Goodwin-Johansson, S.M. Bobbio, C.A. Bartlett, L.N. Yadon., “Integrated force arrays: theory and modelling of static operation”, Journal of micro electromechanical systems, Vol 24, N° 3, September 1995, pp 139-149.

[5] Z. Ren, “Comparison of different force calculation methods in 3D finite element modelling”, IEEE transaction on magnetics, Vol. 30, N°5, September 1995, pp 3471-3474.

[6] F.X. Zgainski, J.L. Coulomb, Y. Maréchal. “A tool for 3-D mesh generation in electromagnetism and electromechanical engineering”, IEEE Transaction on magnetics, Vol 32, N°3, May 1996, pp 1341-1343.

[7] S. Bobbio, F. Delfino, P. Girdinio, P. Molfino, “Equivalent sources methods for the numerical evaluation of magnetic force with extension to nonlinear materials”, IEEE Transaction on magnetics, Vol. 36, N°4, July 2000, pp 663-666

[8] G.S. Park, S.H. Park, “Determination of the curvature of the magnetic fluid under the external forces“, In Proceeding of the COMPUMAG 2001 conference, Evian (France), July 2001.

[9] O. Barré, P. Brochet, “Discrimination of stress formulae induced by magnetic field from experimentation and numerical simulation”, In *Proceedings of the 6th international symposium on electric and magnetic field, EMF’ 2003*, Aachen , October 2003, pp 277-278.

[10] A. Bossavit, "Forces inside a magnet”, *ICS Newsletter*, ISSN 1026-0854, Vol 11 N°1, March 2004, pp 4-12.

[11] F. Henrotte, H.Vande Sande, G. Deliége, K. Hameyer, “Electromagnetic force density in a ferromagnetic material”, IEEE transaction on magnetics”, Vol 40, N°2, March 2004, pp 553-556.

[12] O. Barré, P. Brochet, M. Hecquet, “Experimental validation of magnetic and electric local force formulations associated to energy principle“, In Proceeding of the COMPUMAG 2005 conference, in Shenyang, Liaoning, (China), 26-30 June 2005.